Theor. Appl. Climatol. 58, 105–112 (1997)

Theoretical and Applied Climatology

Center of Studies in Resources Engineering, Indian Institute of Technology, Powai, Bombay, India

Investigation of Drought Through Digital Analysis of Satellite Data and Geographical Information Systems

T. K. Ghosh

With 6 Figures

Received June 12, 1995
Revised August 26, 1996

Summary

This is a study of drought in the arid to semiarid Shahpur and Shorapur areas, of Gulbarga district in Karnataka State, India. IRS-1A LISS 2 data for April, May, and June in 1988 and 1991, and November and December in 1990 and January in 1991 have been analysed to generate albedo and vegetation indices. Rainfall data for a period of 70 years (1922–1991) at 22 stations were used to define isohyetal maps. Soil moisture was calculated using meteorological equations. The Survey of India topomap was used as input for slope analysis. The data surfaces were studied together with the aid of a geographical information system and the final output was produced in the form of a raster image to high-light the different degrees of severity of drought in the region.

1. Introduction

A drought is designed as an anomalously long period of dry weather. It however, differs from aridity, which is a perennial state of water shortage to which life and human settlement might have adapted. Semi-arid regions are most prone to the damaging effects of drought because the demand and the supply of water is critically balanced and in addition the regions suffer ever increasing anthropogenic pressure. The Shahapur-Shorapur study area between 16°30′ and 16°45′ N and 76°40′ and 77°00′ E in Gulbaraga district of Karnataka State, India, is one such semi-arid region (Fig. 1). The study area covers a geographical area of 670 km^2. The area receives a mean annual rainfall between 500 mm and 1000 mm and most of the rainfall occurs between July and September. Between the 1971 and 1981 census, the density of human population per square kilometer increased by 24%. In this paper, the digital analysis of satellite data (IRS-1A LISS 2) and the use of a geographical information system (GIS) are discussed for investigating drought. Integration of data from different sources is not a new development, however, in this study the primary thrust is to produce digital data products for drought investigation by combining data from various sources with widely different characteristics. Strahler et al. (1978) studied vegetation cover with greater accuracy incorporating topographic and other ancillary information. Shelton and Estes (1981) described the integration of Remote Sensing and GIS for decision making. Marble et al. (1983) considered the use of GIS for a large volume of user defined spatial data and display of the end product as the user designed it. Loveland and Johnson (1983) showed that spatial and remotely sensed data may provide a unique look at the past, present and future characteristics of irrigation development. Beran and Rodier (1985), Oladipo (1985), Rao and Subramaniam (1985) and Rao et al.

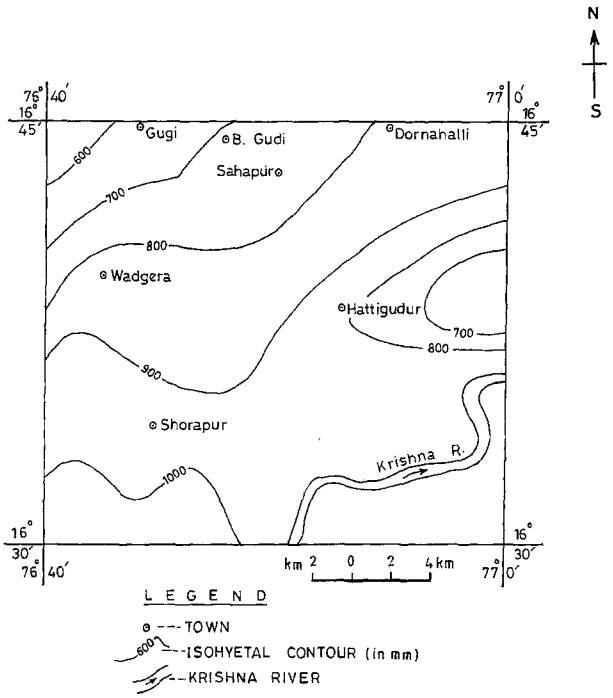

Fig. 1. Location of the study region with mean annual precipitation (Isohyetal map)

(1988) designed drought classification with meteorological parameters. Ripple (1985) showed a relationship between Landsat-TM bands and grass canopy variables. Walsh (1987) studied the drought conditions by integrating NOAA AVHRR and meteorological data. Everitt et al. (1987) presented a study on colour infrared aerial photography with computer aided image processing for detecting drought stress of grasses. Graetz et al. (1988) showed the Landsat measurements of vegetation cover in a semiarid shrub rangeland from 1981 to 1984. The data were integrated into a GIS to assess and monitor the behaviour of individual rangeland types and pastoral properties over the 1981 to 1984 period. Kennedy (1989) provided atmospherically corrected NDVI for monitoring grazing lands in Tunisia. Star et al. (1991) developed improved techniques to integrate Remote Sensing with GIS. Dobson (1992) showed a conceptual framework for integrating Remote Sensing, GIS and Geography. Ghosh (1993) outlined a desertification study integrating Remote Sensing and GIS. Smith and Vidmar (1994) explained the use of Remote Sensing and GIS for developing urban hydrological models.

Meteorological data have been the traditional means for monitoring drought conditions. However such an approach in this semiarid region is not feasible because of very low number of rainfall stations. In this study we examine: (a) the analysis of multitemporal satellite data for generating changes in albedo and in vegetation, (b) the analysis of meteorological data for identifying a change in soil moisture and (c) the use of GIS for integrating satellite based indicators with meteorological based indicators in order to define the severity of drought.

2. Data and Methodology

2.1 Data Acquisition

The IRS-1A LISS 2 (Indian Remote Sensing Satellite-1A Series Linear Imaging Self-Scanning Sensors 2) data sets were obtained over the study area for the dry season (April to June) and for the growing period (November to January) of 1988, 1990 and 1991 from National Remote Sensing Agency, Hyderabad, India. IRS-1A provides data on the same region at intervals of 22 days (the characteristics of IRS data are given in Appendix 1). The dates were chosen according to the constraints of being close to each other and free from any cloud cover. A Colour Composite of an IRS-LISS 2 Image covering the study area is shown in Fig. 2.

70 years of continuous rainfall data, both monthly and annual (1922–1991), were obtained for 22 stations distributed over the study area. The rainfall data were acquired from the Statistical Department, Karnataka State, India.

2.2 Data Processing System

The digital analysis of LISS-2 data covering the area was carried out using a DIPIX image processing system configured around a VAX 11/780 computer system, housed in *CSRE*, Indian Institute of Technology, Bombay. A video capturing interactive digitizer (EIKONIX image scanning system) is also connected with the DIPIX system. An inhouse GIS package is also housed in CSRE.

Fig. 2. IRS-1A-LISS 2 Black & White Composite-covering study area; Path 27, Row 56, 27 April 1988

2.3 Data Analysis and Results

The analysis was carried out in two parts. The first part was the analysis of IRS-1A LISS-2 data and the meteorological data, and the second part involved the use of GIS for defining drought severity.

2.4 Digital Analysis of Satellite Data

The acquired IRS-LISS 2 data sets were first corrected for atmospheric factors (Aranuvachapun, 1983). The corrected data were then displayed on the DIPIX Image Processing System. The control points were selected in order to geographically reference the data with respect to the Survey of India Topo Maps. The georeferenced data had 1 pixel accuracy. The IRS-LISS 2 data sets were aggregated to a 36.25m $\times$ 36.25m cell size. A neighbourhood approach was utilised to georeference the data. For example, a 3×3 pixel window is used and the centre pixel's digital number (DN) would be the average value of the 9 pixels.

2.5 Albedo Index

Otterman and Fraser (1976) described a method for the calculation of reflectance of terrain features from atmospherically corrected Landsat MSS data. The surface albedo measurement is based on summing up the radiances in each band of the satellite data. Spectral Albedo (A_s) is here taken as the ratio of reflected

to incident spectral radiance in the visible range of satellite data. The radiance (R) is calculated as $= D_n/D_{\max}(L_{\max} - L_{\min}) + L_{\min}$, where D_n = pixel's digital number, $D_{\max}$ = maximum digital value in the dynamic range, $L_{\max}$ = maximum saturation radiance measured by the detector and $L_{\min}$ = minimum saturation radiance measured by the detector. The detector calibration factors were obtained from the Data User Handbook of the Satellite Sensor. From the IRS-LISS 2 data an albedo image was derived. The wavelength integrated albedo is an additive function (Robinove 1981) and is accordingly calculated here as Albedo $(A_s) = \frac{\pi}{E \sin\theta} \times$ (Radiance sum in four wavebands). Where E is the irradiance at the top of the atmosphere, θ is the solar elevation angle. The albedo for each pixel was computed. The maximum albedo for each pixel was obtained by summing up the albedos during the dry months (April to June) and the minimum albedo for each pixel was obtained by summing up all the albedos during the growing season (November to January). In order to obtain a drought index and its variation, the dry period maximum was subtracted from the growing period minimum. The difference is taken here as a measure of drought. The minimum albedo differences (7.22 after subtraction) were given the numerical value 1 and the maximum difference (28.29 after subtraction) the numerical value 9, thus the value 5 represents mean conditions. The differences were calculated for all pixels.

2.6 *Vegetation Index*

The reflectivities in the red (channel 3) and the near infrared (channel 4) spectral region were used to compute the normalised difference vegetation index (NDVI) like those obtained from NOAA data (Kennedy, 1989).

$$\text{Vegetation Index} = \frac{\text{Channel 4 reflectivity} - \text{Channel 3 reflectivity}}{\text{Channel 4 reflectivity} + \text{Channel 3 reflectivity}}$$

The maximum vegetation index for each pixel was obtained by summing up the vegetation index values during the growing months (November to January) and the minimum vegetation index was obtained by summing up the vegetation index values during the dry months (April to June). To examine the drought period the growing period maximum vegetation index was subtracted from the dry period minimum. The difference is a drought measure, where the minimum vegetation index difference (0.02) was given the numerical value 9, the maximum difference (0.82) the value 1. The whole vegetation index difference scene was expanded into a 0 to 255 grey level image. The difference image is shown in Fig. 3.

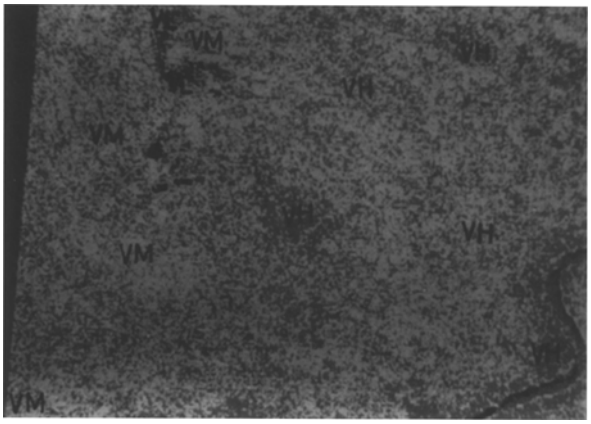

Fig. 3. Vegetation index difference image. *VH* High/dense vegetation; *VM* Moderate vegetation; *VL* Scarce vegetation

2.7 *Landuse/Landcover Class Analysis*

A landuse/landcover image was obtained by analysing satellite data (using FCC, supervised classification and the Survey of India Topo Map). The image was properly registered with the pixel/cell size 36.25 m × 36.25 m. The image was taken as another GIS data surface (Fig. 4). 9 was assigned to the class of stony and sandy surfaces, 5 to fallow land on red soil and 1 to fallow land on black soil. If any pixel was occupied by multiple classes, the pixel's numerical value was determined by calculating the mean of all classes occupying the pixel.

2.8 *Meteorological Data Analysis*

70 years of continuous rainfall data for 22 stations were used to construct the isohyetal map (Fig. 1). The average rainfall for an area/cell was computed by interpolating linearily between

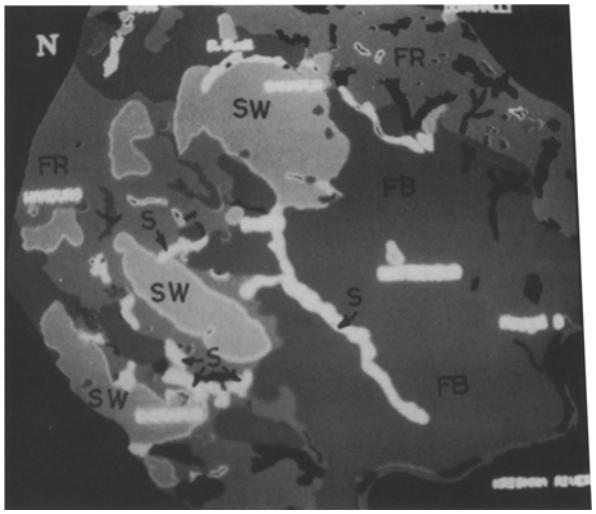

Fig. 4. Landuse/landcover image. *FB* Fallow land on black soil; *FR* Fallow land on red soil; *SW* Stony wastes; *S* Sandy regions

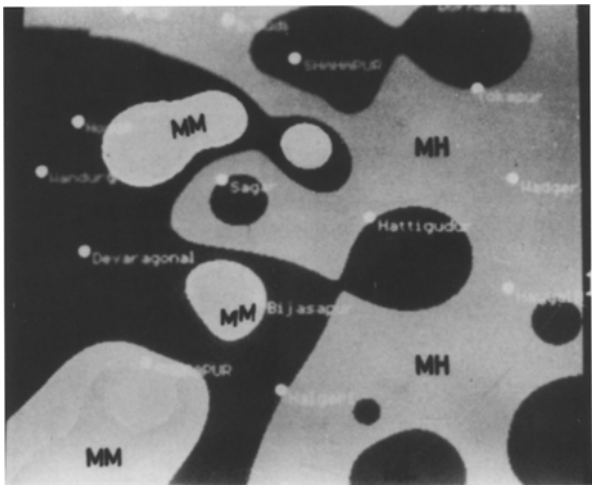

Fig. 5. Soil moisture difference image. *MH* Area of high soil moisture; *MM* Area of moderate soil moisture; *ML* Area of low soil moisture

contours. The area of each cell was aggregated to 36.25 m × 36.25 m. A graphic digitizer was used to obtain the coordinates of each cell.

2.9 Soil Moisture Analysis

Soil samples were collected at all 22 stations. A soil moisture estimate was calculated based on the formula:

$$S = K(S_{j-1} + P_{j-1})$$

where S = soil moisture, P_{j-1} = Previous month's accumulated rainfall S_{j-1} = Previous month's accumulated soil moisture and K = coefficient, expressed as

$$K = e^{-1.33} \times E_p,$$

with E_p = potential evaporation (Owe et al., 1988). The initial soil moisture values as well as the potential evaporation were obtained from the Area Development Authority-Upper Krishna Project (CADA-UKP), Gulbarga, Karnataka State, India. For example on a black soil, the potential evaporation (moisture storage capacity) for a 5 year average was measured as 0.2096 m, the previous month's accumulated soil moisture for a 5 year average was measured as 13.8% and the previous month's accumulated precipitation for a 5 year average was measured as 39.9 mm (CADA-UKP Records) and the soil moisture for the month as calculated was 40.63%.

The maximum soil moisture was obtained by summing up all the soil moisture values during the growing months (November to January) and the minimum soil moisture was obtained by summing up all the soil moisture values during the dry months (April to June). To examine the drought period and variability within the growing period the maximum was subtracted from the dry period minimum. The difference is a measure of drought where the minimum soil moisture difference (0.13) was assigned a value of 9, the maximum (0.84) a value of 1 and 5 for the mean. The soil moisture contour lines were plotted and average soil moisture for each cell was computed by interpolating between the contour lines. The area of each cell was aggregated to 36.25 m × 36.25 m. A graphic digitizer was used to set the co-ordinates for each cell. Using the point attributes for spatial interpolation (using the inverse square method), a soil moisture difference image was formed (Fig. 5). The image was entered as a further GIS surface, properly co-registered with the albedo and vegetation images.

2.10 Slope Data Analysis

The mean topographic slope was derived from the Survey of India, Topo Map, on a scale 1:50,000. The slope isolines were entered into the DIPIX image processing system as another

GIS surface. The slope of the terrain varied between 0.01 and 0.28. A numerical value 1 was assigned to slope 0.01, 9 to 0.28 and 5 to the mean. While calculating the vegetation index from the IRS-LISS 2 data, it was observed that the density of vegetation between valleys and hilly terrain changed strongly. In addition, it was found that soil moisture was higher in the valleys and less on the hills. Slope factors are therefore very important.

2.11 Data Integration in GRAM-GIS

All the different types of data were standardised before using them for any kind of analysis. The standardisation of the data was carried out by reformatting, rescaling, integration and finally, map generation.

GRAM is a Georeferenced Area Management system that has been developed in the Centre of Studies in Resources Engineering, Indian Institute of Technology, Powai, Bombay, India. It is a raster based GIS.

The data surfaces were geometrically corrected and co-registered properly with ground control points. Overlaying of the data surfaces was performed along the lines of Jensen (1986). For example, if a particular pixel/cell has value 9 on the vegetation image, 1 on the slope image, 5 on the albedo image, 9 on the soil moisture image and 9 on a landuse/landcover image, the composite value for that pixel becomes, $9 + 1 + 5 + 9 + 9 = 33$. The composite values (index) for all pixels/cells were determined and normalised to a grey scale of 0 and 255. A final image was obtained after the user had defined the classification range. This image is named a drought watch and it indicates the pixel values of different relative importance. The results of the drought watch are given in Table 1. A final iso-line drawing of the drought watch (328 × 350 pixels) is shown in Fig. 6. The results were,

Table 1. *Description of Drought Measure*

Composite drought index	Grey level range (0–255 scale)	Drought condition
35 or above	>155	Severe drought
25 to 34	125 to < 155	Moderate drought
15 to < 25	81 to < 125	Mild drought
up to 14	up to 80	No drought

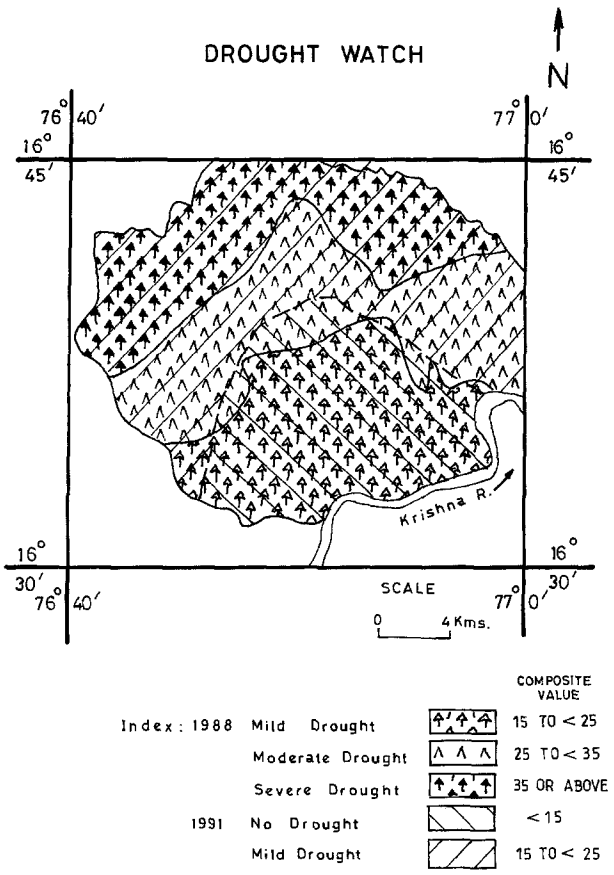

Fig. 6. Drought severity map

however, compared in the field with the actual droughts in 1988 and 1991 and it was found that the results agreed well. 3 locations were selected in the field: near Hattigudur; near Shorapur; and near Sahapur (Fig. 1). The ratio value P/PET, (where P is the annual precipitation and PET is the annual potential evapotranspiration) was measured as 0.52 and above near Hattigudur, 0.33 and < 0.52 near Shorapur, and < 0.33 near Sahapur. The area near Hattigudur experienced mild drought, the area near Shorapur experienced moderate drought and the area near Sahapur experienced severe drought.

This overall agreement was seen as justification for the simple approach adopted here of just adding the numerical values assigned to the different drought indicating parameters like vegetation index, slope, albedo, soil moisture and land cover. Only if more quantitative field observations on drought severity would be available, would the investment in a varied approach be justified.

3. Discussion

The vegetation index computed in this study from IRS-1 A LISS 2 satellite data are sensitive to the state of vegetation like the normalised difference vegetation index obtained from NOAA data. The vegetation index varied from 0.03 to 0.82. Analysis of the IRS 1A LISS 2 data led to the computation of an albedo (A_s) index. Data for this study varied from 7.22 to 28.29. The soil moisture data, as calculated for this study area based on the meteorological data, varied between 0.13 and 0.48. Change of slope in the terrain also influences the vegetation, albedo and soil moisture index data. For example, in the valley, the vegetation index was high, albedo was low and there was more surface moisture. However, in hilly terrain the situation was completely reversed. While analysing the land-use/landcover image the stony and sandy areas also showed low soil moisture status. The topographic slope that was derived from the Survey of India Topo Map varied from 0.01 to 0.28 for this study area.

All the GIS data surfaces were properly co-registered with their respective cell's co-ordinates. Each cell's (36.25 m × 36.25 m) composite drought index was obtained. The composite drought index was strongly varying from below 15 to 35 and above. The drought index values were transferred into a grey scale with values from 0 to 255. The composite index 35 or above, indicated by the grey level range class above 155, showed severe drought, while an index between 25 and < 35, indicated by the grey level range between 125 and < 155, was classified as moderate drought. The composite drought index between 15 and < 25, indicated by the corresponding grey level range between 81 and < 125, was classified as mild drought and the composite drought index < 15, indicated by the corresponding grey level range up to 80, was classified as no drought.

Aurangabad and Parbhani, the two drought prone districts of Maharashtra State, India were selected as two field sites to test the results of the composite drought indices obtained through the combination of several parameters. Both the test sites indicated the same composite drought index, as obtained for this study.

4. Conclusion

Analysis of atmospherically corrected IRS-1A LISS 2 data for the dry season (April to June) and growing (November to January) seasons in 1988, 1990 and 1991, meterological data and slope data all integrated in a GIS have produced interesting and encouraging results on drought severity. A composite drought index derived from the combined analyses can provide a useful tool for investigation, monitoring and prediction of drought. The spatial variations of droughts have been identified in 1988 and 1991 drought watches. The GIS approach allows planners and managers to analyse alternatives during drought conditions. Future work will concentrate on attempting to utilise more GIS data surfaces to determine drought conditions.

Acknowledgements

The author is thankful to the Head of the Centre of Studies in Resources Engineering, Indian Institute of Technology, Bombay, India, for his constant encouragement while conducting this work. The author also wishes to acknowledge Shri G. K. Tripathy for providing some field and technical assistance. This work was made possible by a research grant of the Government of India.

Appendix 1

IRS-1A Indian Remote Sensing Satellite Imaging Sensors Characteristics

	Linear imaging self scanning sensors, LISS 1	Linear imaging self scanning sensors LISS 2
Focal length (mm)	162.2	324.4
Field-of-view (deg)	9.4	4.7+4.7
Instantaneous field of view, IFOV (microrad)	80.0	40.0
Detector	2048 elements CCD	2048 elements CCD
Ground resolution (meter)	72.5	36.25
Spectral range (μm)	0.45–0.86	0.45–0.86
Number of bands	4	4
Swath (kms)	148	74 × 2
Radiometric resolution (grey levels)	128	128

References

Aranuvachapun, S., 1983: Variation of atmospheric optical depth for remote sensing radiance calculations. *Remote Rensing Environ.,* **13**, 131–147.

Beran, M. A., Rodier, J. A., 1985: Hydrological aspects of drought. A contribution to the International Hydrological Programme, Uensco WMO, **39**, 65–85.

Dobson, J. E., 1993: Commentary: A conceptual framework for integrating remote sensing, GIS and geography. *Photogrammetric Engineering & Remote Sensing,* **59**, 1491–1496.

Everitt, J. H., Escobar, D. E., Alaniz, M. A., Hussey, M. A., 1987: Drought-stress detection of buffelgrass with colour-infrared aerial photography and computer-aided image processing. *Photogrammetric Engineering & Remote Sensing,* **53**, 1255–1258.

Ghosh, T. K., 1993: Environmental impacts analysis of desertification through remote sensing and land based information system. *J. Arid Environments,* **25**, 141–150.

Graetz, R. D., Pech, R. P., Davis, A. W., 1988: The assessment and monitoring of sparsely vegetated rangelands using calibrated Landsat data. *Int. J. Remote Sensing,* **9**, 1201–1222.

Jensen, J. R., 1986. *Introductory Digital Image Processing – A Remote Sensing Perspective*. New Jersey: Prentice-Hall, Chapter 10, pp. 254–271.

Kennedy, P. J., 1989: Monitoring the phenology of Tunisian grazing lands. *J. Int. Remote Sensing,* **10**, 835–845.

Loveland, R. T., Jhonson, E. G., 1983: The role of remotely sensed and other spatial data for predictive modelling. The Umatilla, Oregon, Example. *Photogrammetry Engineering & Remote Sensing*, **49**, 1183–1192.

Marble, D. F., Penquet, D. J., Boyle, A. R., Bryant, N., Calkins, H. W., Johnson, T., Zobrist, A., 1983: Geographic information systems and remote sensing. In: Colwell, R.N. (ed.) *The Manual of Remote Sensing*. Falls Church, Virginia. American Society of Photogrammetry, Vol. **1**, 923–958.

Otterman, J., Fraser, R. S., 1976: Earth-atmospheric system and surface reflectivities in arid regions from Landsat MSS data. *Remote Sensing Environ.,* **5**, 247–266.

Owe, M., Chang, A., Golus, R. E., 1988: Estimating surface soil moisture from satellite microwave measurements and a satellite derived vegetation index. *Remote Sensing Environ.,* **24**, 331–345.

Oladipo, E. O., 1985: A comparative performance analysis of three meteorological drought indices. *J. Climatol.,* **5**, 655–664.

Rao, A. S., Subramaniam, A. R., 1986: An analysis of droughts in Maharashtra by a modified Palmer's approach. *Manusai,* **37**, 377–384.

Rao, V. B., Satyamurty, P., De Brito, J. I. B., 1986: On the 1983 drought in North-East Brazil. *J. Climatol.,* **6**, 43–51.

Ripple, W. J., 1985: Landsat thematic mapper bands for fescue grass vegetation. *Int. J. Remote Sensing,* **6**, 1373–1384.

Rovinove, C. J., 1981: Arid land monitoring using Landsat albedo difference image. *Remote Sensing Environ.,* **11**, 133–156.

Shelton, R. C., Estes, J. E., 1981: Remote sensing and geographical information systems: an unrealised potential. *Geoprocessing,* **1**, 395–430.

Smith, B. M., Vidmar, A., 1994: Data set derivation for GIS-based urban hydrological modelling. *Photogrammetric Engineering & Remote Sensing,* **60**, 67–76.

Star, J. L., Estes, J. E., Davis, F. W., 1991: Improved integration of remote sensing and geographic information systems. *Photogrammetric Engineering & Remote Sensing,* **57**, 643–645.

Strahler, A. H., Logan, T. L., Bryant, N. A., 1978: Improving forest cover classification accuracy from Landsat by incorporating topographic information. Proceedings: Twelfth International Symposium on Remote Sensing of the Environment. Ann Arbor, Michigan: Environmental Research Institute, pp. 927–942.

Author's address: T. K. Gosh, Centre of Studies in Resources Engineering, Indian Institute of Technology, Powai Bombay 400 076, India.